

# Instanton contributions to Wilson loops with general winding number in two dimensions and the spectral density

A. Bassetto<sup>1</sup>, L. Griguolo<sup>2</sup> and F. Vian<sup>1</sup>

<sup>1</sup>*Dipartimento di Fisica "G. Galilei", INFN, Sezione di Padova,  
Via Marzolo 8, 35131 Padua, Italy*

<sup>2</sup>*Dipartimento di Fisica "M. Melloni", INFN, Gruppo Collegato di Parma,  
Viale delle Scienze, 43100 Parma, Italy*

## Abstract

The exact expression for Wilson loop averages winding  $n$  times on a closed contour is obtained in two dimensions for pure  $U(N)$  Yang-Mills theory and, rather surprisingly, it displays an interesting duality in the exchange  $n \leftrightarrow N$ . The large- $N$  limit of our result is consistent with previous computations. Moreover we discuss the limit of small loop area  $\mathcal{A}$ , keeping  $n^2\mathcal{A}$  fixed, and find it coincides with the zero-instanton approximation. We deduce that small loops, both at finite and infinite "volume", are blind to instantons. Next we check the non-perturbative result by resumming 't Hooft-CPV and Wu-Mandelstam-Leibbrandt (WML)-prescribed perturbative series, the former being consistent with the exact result, the latter reproducing the zero-instanton contribution. A curious interplay between geometry and algebraic invariants is observed. Finally we compute the spectral density of the Wilson loop operator, at large  $N$ , via its Fourier representation, both for 't Hooft and WML: for small area they exhibit a gap and coincide when the theory is considered on the sphere  $S^2$ .

DFPD 99/TH 23

UPRF-99-08

PACS numbers: 11.15Bt, 11.15Pg, 11.15Me

Keywords: Two-dimensional QCD, instantons, Wilson loops.

## I. INTRODUCTION

The non-perturbative structure of non-abelian quantum gauge theories is still a challenging topic in spite of a large amount of efforts in this direction. Whereas perturbation theory provides a well-established computational tool to describe the weak coupling regime, quantitative predictions for the behaviour of the strongly-coupled theory are extremely hard to be found. In the last few years much attention has been devoted to derive exact results in the supersymmetric case, by exploiting duality properties [1,2]. Nevertheless we believe a “traditional” field theory approach is appealing, most of all in comparing perturbative and non-perturbative aspects.

In particular this approach becomes crucial in the light-front formulation of quantum gauge theories [3]: though some non-perturbative features are thought to be transparent, a consistent framework in the continuum is still lacking. Moreover the relation with the usual perturbative equal-time quantization remains unclear.

Such problems have recently been tackled in the simplified context of two-dimensional gauge theories ( $YM_2$ ), taking advantage of the lattice solutions [4]. As far as the continuum is concerned, in two dimensions the theory seems trivial when quantized in the light-cone gauge. As a matter of fact, in the absence of dynamical fermions, it looks indeed free, being described by a Lagrangian quadratic in the fields.

Still topological degrees of freedom occur if the theory is put on a (partially or totally) compact manifold, whereas the simpler behaviour enforced by the light-cone gauge condition on the plane entails a severe worsening in its infrared structure. These features are related aspects of the same basic issue: even in two dimensions the theory contains non trivial dynamics, as immediately suggested by other gauge choices as well as by perturbative calculations of gauge invariant quantities, typically of Wilson loops [5]. One can say that, in light-cone gauge, dynamics gets hidden in the very singular nature of correlators at large distances (IR singularities).

The first quantity that comes to mind is the two-point correlator. If the theory is

quantized in the gauge  $A_- = 0$  at *equal-times*, the free propagator has the following causal expression (WML prescription) in two dimensions

$$D_{++}^{WML}(x) = \frac{1}{2\pi} \frac{x^-}{-x^+ + i\epsilon x^-}, \quad x^\pm = \frac{x^0 \pm x^1}{\sqrt{2}}, \quad (1)$$

first proposed by T.T. Wu [6]. In turn this propagator is nothing but the restriction in two dimensions of the expression proposed by S. Mandelstam [7] and G. Leibbrandt [8] in four dimensions and derived by means of a canonical quantization in ref. [9]. In the equal-time formulation, the causal behaviour is induced by the propagation of unphysical degrees of freedom (probability ghosts), which can be expunged from the “physical” Hilbert space, but still contribute in intermediate lines as timelike photons do in the QED Gupta-Bleuler quantization.

In dimensions higher than two, where “physical” degrees of freedom are switched on (transverse “gluons”), this causal prescription is the only acceptable one; indeed causality is mandatory in order to get correct analyticity properties, which in turn are the basis of any consistent renormalization program [10]. It has been shown in perturbative calculations [11] that agreement with Feynman gauge results can only be obtained if a causal propagator is used in light-cone gauge.

The situation is somewhat different in exactly two dimensions. Here the theory can be quantized on the *light-front* (at equal  $x^+$ ); with such a choice, no dynamical degrees of freedom occur as the non-vanishing component of the vector field does not propagate

$$D_{++}^P(x) = -\frac{i}{2}|x^-|\delta(x^+), \quad (2)$$

but rather gives rise to an instantaneous (in  $x^+$ ) Coulomb-like potential. On the other hand, renormalization is no longer a concern for a pure Yang-Mills theory in two dimensions.

A formulation based essentially on the potential in Eq. (2) was originally proposed by G. 't Hooft in 1974 [12], to derive beautiful solutions for the  $q\bar{q}$ -bound state problem under the form of rising Regge trajectories.

When inserted in perturbative Wilson loop calculations, expressions (1) and (2) lead to completely different results, as first noticed in ref. [5]. The origin of this discrepancy

was eventually understood in ref. [13], where it was shown that genuine non-perturbative excitations (“instantons”) are necessary in the equal-time formulation (Eq. (1)) in order to obtain the exact result, which in turn is easily recovered in the light-front formulation (Eq. (2)) just by summing the perturbative series. This surprising feature strengthens the belief that the light-front vacuum may indeed be much simpler than the one in the equal-time formulation, at least in two dimensions.

In order to gain a deeper insight in the different physics described by either ’t Hooft or WML prescription, we have decided to study a wider class of loops, *i.e.* loops winding around themselves an arbitrary number of times. Actually, their knowledge appear to be intimately related [14] to the general solution of the Makeenko-Migdal equations at large  $N$  [15]. Furthermore, in the large- $N$  limit, the spectral density of the eigenvalues of the Wilson operator is completely determined in terms of such loops. Remarkably this spectral density carries non-trivial information about the master field [16] of the theory even on the plane. Therefore it seems natural to explore winding loops using both the perturbative WML prescription and the ’t Hooft one in order to understand whether instanton effects are still able to distinguish between the two.

In Sect. II we start by deriving Wilson loops at finite  $N$  and arbitrary  $n$  on the plane from the non-perturbative solution on the sphere  $S^2$ . To our knowledge an explicit formula, obtained by decompactification, appears in literature for the first time and extends previous results limited to a small number of windings [17,18]. It contains all instanton contributions and turns out to correspond to the exact resummation of the perturbative series defined via ’t Hooft propagator. Once again light-front quantization seems to capture the correct vacuum of the theory. On the other hand, by isolating the zero-instanton contribution on the sphere, we end up with the perturbative resummation of WML expressed in terms of a Laguerre polynomial. Hence the picture is fully consistent with our previous investigations [13,19].

Having the general expression for a Wilson loop of  $U(N)$  with  $n$  windings, we are enabled to perform different limits covering complementary regimes of the theory. First of all, in

the large- $N$  limit with  $g^2N$  fixed, we recover the well-known result of [17,20] in terms of a Laguerre polynomial. Surprisingly enough, taking instead  $n$  to infinity and keeping  $n^2\mathcal{A}$  fixed, the perturbative result of WML is reproduced. We can explain the latter behaviour by observing that, having the instantons a finite size, small loops are essentially blind to them. This also teaches us, as we will investigate further in the sequel, that a remnant of the weak phase on the sphere survives the decompactification limit. In fact one can as well study the same limit directly at finite total area and what is found is precisely the zero-instanton contribution. The parallelism of the limits  $N \rightarrow \infty$  and  $n \rightarrow \infty$ , reflected by the same functional form, has to be ascribed to the symmetry of the general formula for the Wilson loop under the exchange  $N \leftrightarrow n$ , up to a rescaling of the area.

The next step consists in computing the same quantities by means of the perturbative expansion. This is not simply a check of the correctness of the previous interpretation, but also casts light on the interplay between geometry and colour in the different prescriptions, and is done in Sect. III. Whereas for WML the resummation of the full perturbative series is a straightforward generalization of the computation performed in [21] for  $n = 1$ , the analog with 't Hooft unveils the full non-abelian character of such a prescription. Due to its complexity, we have restricted ourselves to the calculation of the Wilson loop with winding  $n$  to  $\mathcal{O}(g^4)$ : as we will see, at this level already a large amount of classes of diagrams need being considered. As a matter of fact, we have realized that adopting WML all the diagrams contributing to a given perturbative order entails the same geometrical factor, so that only the structure of the colour traces is relevant. Fortunately the sum of the colour factor is encoded in the matrix integral of [21]. At variance with WML, 't Hooft prescription leads to different geometrical integrals for different classes of graphs, which, together with the colour traces, complicate the resummation of the perturbative series. Still, in this framework we have been able to describe the mechanism underlying both the limits  $N \rightarrow \infty$  and  $n \rightarrow \infty$ . It is rather amusing to observe how the latter limit precisely selects a class of diagram whose geometrical factor is the same as in WML, explaining in this case the perturbative resummation with WML. When performing the former limit the situation is

trivial from an algebraic point of view (only non-crossed diagrams contribute), while the sum over geometrical factors is quite involved. We have evaluated it by exploiting the symmetry under the exchange  $N \leftrightarrow n$ , which shows a curious interplay between geometry and the algebraic invariants.

Finally in Sect. IV we have applied previously derived results to the computation of the spectral function in the large- $N$  limit. In the 't Hooft case the situation is well-known [16,22], a gap appears when the area of the loop is below a critical value, resembling the weak-phase behaviour of the same quantity on the sphere. The novelty comes out with WML, for which a gap was expected at any value of the area, since instanton excitations should be neglected. On the contrary the gap is present only for sufficiently small loops and, in this case, again the density coincides with the same quantity on the sphere in the weak phase.

Conclusions are drawn in Sect. V, whereas technical details are deferred to Appendices A and B.

## II. THE WILSON LOOP WITH WINDING NUMBER $n$

Our starting point are the well-known expressions [4] of the exact partition function and of a Wilson loop with winding number  $n$  for a pure  $U(N)$  Yang-Mills theory on a sphere  $S^2$  with area  $A$

$$\mathcal{Z}(A) = \sum_R (d_R)^2 \exp \left[ -\frac{g^2 A}{4} C_2(R) \right], \quad (3)$$

$$\begin{aligned} \mathcal{W}_n(A - \mathcal{A}, \mathcal{A}) &= \frac{1}{\mathcal{Z}_N} \sum_{R,S} d_R d_S \exp \left[ -\frac{g^2(A - \mathcal{A})}{4} C_2(R) - \frac{g^2 \mathcal{A}}{4} C_2(S) \right] \\ &\times \int dU \text{Tr}[U^n] \chi_R(U) \chi_S^\dagger(U), \end{aligned} \quad (4)$$

$d_{R(S)}$  being the dimension of the irreducible representation  $R(S)$  of  $U(N)$ ;  $C_2(R)$  ( $C_2(S)$ ) is the quadratic Casimir,  $A - \mathcal{A}, \mathcal{A}$  are the areas singled out by the loop, the integral in (4)

is over the  $U(N)$  group manifold and  $\chi_{R(S)}$  is the character of the group element  $U$  in the  $R(S)$  representation. We immediately notice that  $\mathcal{W}_n = \mathcal{W}_{-n}$ .

Eqs. (3), (4) can be easily deduced from the solution of Yang-Mills theory on the cylinder, using the fact that the hamiltonian evolution is governed by the laplacian on  $U(N)$ : we call Eqs. (3),(4) the heat-kernel representations of  $\mathcal{Z}(A)$  and  $\mathcal{W}_n(A - \mathcal{A}, \mathcal{A})$ , respectively.

In order to evaluate  $\mathcal{W}_n(A - \mathcal{A}, \mathcal{A})$  in the decompactification limit we write them explicitly for  $N > 1$  in the form

$$\begin{aligned} \mathcal{Z}(A) &= \frac{1}{N!} \exp \left[ -\frac{g^2 A}{48} N(N^2 - 1) \right] \sum_{m_i=-\infty}^{+\infty} \Delta^2(m_1, \dots, m_N) \\ &\times \exp \left[ -\frac{g^2 A}{4} \sum_{i=1}^N \left( m_i - \frac{N-1}{2} \right)^2 \right], \end{aligned} \quad (5)$$

$$\begin{aligned} \mathcal{W}_n(A - \mathcal{A}, \mathcal{A}) &= \frac{1}{\mathcal{Z} N N!} \exp \left[ -\frac{g^2 A}{48} N(N^2 - 1) \right] \\ &\times \sum_{k=1}^N \sum_{m_i=-\infty}^{+\infty} \Delta(m_1 + n \delta_{1,k}, \dots, m_N + n \delta_{N,k}) \Delta(m_1, \dots, m_N) \\ &\times \exp \left[ -\frac{g^2 (A - \mathcal{A})}{4} \sum_{i=1}^N \left( m_i - \frac{N-1}{2} \right)^2 - \frac{g^2 \mathcal{A}}{4} \sum_{i=1}^N \left( m_i - \frac{N-1}{2} + n \delta_{i,k} \right)^2 \right]. \end{aligned} \quad (6)$$

We have described the generic irreducible representation by means of the set of integers  $m_i = (m_1, \dots, m_N)$ , related to the Young tableaux, in terms of which we get

$$\begin{aligned} C_2(R) &= \frac{N}{12} (N^2 - 1) + \sum_{i=1}^N \left( m_i - \frac{N-1}{2} \right)^2, \\ d_R &= \Delta(m_1, \dots, m_N). \end{aligned} \quad (7)$$

$\Delta$  is the Vandermonde determinant and the integration in Eq. (4) has been performed explicitly, using the well-known formula for the characters in terms of the set  $m_i$ .

In this section we will study the partition function (3) and the Wilson loop (4) in the limit of infinite area, by showing they are dominated by particular representations labelled by suitable indices  $\{\hat{m}_i\}$ . Let us suppose  $N$  odd, so that the term  $(N-1)/2$  in the Casimir



operator is integer and can be absorbed in the sum over  $m_i$ <sup>1</sup>

$$C_2(R) = \frac{N}{12}(N^2 - 1) + \sum_{i=1}^N m_i^2. \quad (8)$$

It is now easy to see that the dominant contributions are given by the following set of indices

$$\{\hat{m}_i\} = \left\{ 0, \pm 1, \pm 2, \dots, \pm \frac{N-1}{2} \right\}, \quad (9)$$

with all possible permutations, for which the minimum value of the Casimir is reached and reads

$$C_2(\{\hat{m}_i\}) = \frac{N(N^2 - 1)}{6}. \quad (10)$$

Finally, by exploiting the symmetry, in the large  $A$  limit the partition function becomes

$$\mathcal{Z}(A \rightarrow \infty) = \Delta^2(\hat{m}_1, \dots, \hat{m}_N) \exp \left[ -\frac{g^2 A}{24} N(N^2 - 1) \right]. \quad (11)$$

We now turn to the Wilson loop (6). Thanks to its symmetry, we can always choose  $k = 1$  and the equation becomes

$$\begin{aligned} \mathcal{W}_n(A - \mathcal{A}, \mathcal{A}) &= \frac{1}{\mathcal{Z}} \exp \left[ -\frac{g^2 A}{48} N(N^2 - 1) \right] \sum_{m_i=-\infty}^{+\infty} \Delta(m_1, \dots, m_N) \\ &\times \Delta(m_1 + n, \dots, m_N) \exp \left[ -\frac{g^2 A}{4} \sum_{i=1}^N m_i^2 - \frac{g^2 \mathcal{A}}{4} (n^2 + 2nm_1) \right]. \end{aligned} \quad (12)$$

When the previous formula is evaluated in the decompactification limit  $A \rightarrow \infty$ ,  $\mathcal{A}$  fixed, that is for  $\{m_i\} = \{\hat{m}_i\}$ , we get

$$\mathcal{W}_n(\mathcal{A}; N) = \frac{\exp \left[ -\frac{g^2 \mathcal{A}}{4} n^2 \right]}{N!} \sum_{\{\hat{m}_i\}} \frac{\Delta(\hat{m}_1 + n, \dots, \hat{m}_N)}{\Delta(\hat{m}_1, \dots, \hat{m}_N)} \exp \left[ -\frac{g^2 \mathcal{A}}{2} n \hat{m}_1 \right]. \quad (13)$$

After writing explicitly the Vandermonde determinants and taking into account the symmetry over the indices  $\{\hat{m}_2, \dots, \hat{m}_N\}$  we are left with a nice formula for  $\mathcal{W}_n$

---

<sup>1</sup>If  $N$  is even,  $(N-1)/2$  will be half-integer, but this does not alter our conclusions.

$$\mathcal{W}_n(\mathcal{A}; N) = \frac{1}{N} \exp \left[ -\frac{g^2 \mathcal{A}}{4} n^2 \right] \sum_{k=-\frac{N-1}{2}}^{\frac{N-1}{2}} \exp \left[ -\frac{g^2 \mathcal{A}}{2} n k \right] \prod_{\substack{j=-\frac{N-1}{2} \\ j \neq k}}^{\frac{N-1}{2}} \frac{k+n-j}{k-j}. \quad (14)$$

Remembering that  $\mathcal{W}_0 = 1$  and that  $\mathcal{W}_n$  is even in  $n$ , in the following we shall explicitly consider only positive values of  $n$ .

It is not difficult to show that (14) can be conveniently rewritten as

$$\begin{aligned} \mathcal{W}_n(\mathcal{A}; N) = \frac{1}{nN} \exp \left[ -\frac{g^2 \mathcal{A}}{4} n(N+n-1) \right] \sum_{k=0}^{n-1} \frac{(-1)^k}{k!} \frac{(N+n-1-k)!}{(N-1-k)!(n-1-k)!} \\ \times \exp \left[ \frac{g^2 \mathcal{A}}{2} n k \right] \quad \text{for } N > n, \end{aligned} \quad (15)$$

$$\begin{aligned} \mathcal{W}_n(\mathcal{A}; N) = \frac{1}{nN} \exp \left[ -\frac{g^2 \mathcal{A}}{4} n(N+n-1) \right] \sum_{k=0}^{N-1} \frac{(-1)^k}{k!} \frac{(N+n-1-k)!}{(N-1-k)!(n-1-k)!} \\ \times \exp \left[ \frac{g^2 \mathcal{A}}{2} n k \right] \quad \text{for } N < n, \end{aligned} \quad (16)$$

that can be combined together to produce the general expression

$$\begin{aligned} \mathcal{W}_n(\mathcal{A}; N) = \frac{1}{nN} \exp \left[ -\frac{g^2 \mathcal{A}}{4} n(N+n-1) \right] \sum_{k=0}^{+\infty} \frac{(-1)^k}{k!} \frac{\Gamma(N+n-k)}{\Gamma(N-k)\Gamma(n-k)} \\ \times \exp \left[ \frac{g^2 \mathcal{A}}{2} n k \right]. \end{aligned} \quad (17)$$

The series is actually a finite sum, stopping at  $k = n - 1$  or  $k = N - 1$ , depending on the smaller one. Some comments are now in order. First of all we notice that when  $n > 1$  the simple abelian-like exponentiation is lost. In other words the theory starts to feel its non-abelian nature as the appearance of different ‘‘string tensions’’ makes clear: the Coulomb law is violated and the combinatorial coefficients in (17) are intimately related, as we will see in the following, to the presence of instanton contributions to light-front vacuum. Actually, from the sphere point of view, (17) can be understood as coming from an instantons’ resummation. Indeed, as first noted by Witten [23], it is possible to represent  $\mathcal{Z}(A)$  and  $\mathcal{W}_n(A - \mathcal{A}, \mathcal{A})$  as a sum over unstable instantons, where each instanton contribution is associated to a finite, but not trivial, perturbative expansion. In ref. [13], as confirmed by

the computation on the torus in [19], it was shown that if only the zero-instanton sector is considered, in the decompactification limit one exactly recovers the sum of the perturbative series for  $n = 1$ , in which the light-cone gauge Yang-Mills propagator is WML-prescribed (1). Precisely we had for the zero-instanton case

$$\mathcal{W}_1^{(0)} = \frac{1}{N} \exp \left[ -g^2 \frac{(A - \mathcal{A})\mathcal{A}}{4A} \right] L_{N-1}^{(1)} \left( g^2 \frac{(A - \mathcal{A})\mathcal{A}}{2A} \right). \quad (18)$$

$L_\beta^{(\alpha)}(x)$  being the generalized Laguerre polynomials, reproducing for  $A \rightarrow \infty$  the exact resummation of [21]

$$\mathcal{W}_1^{(0)} = \frac{1}{N} \exp \left[ -\frac{g^2 \mathcal{A}}{4} \right] L_{N-1}^{(1)}(g^2 \mathcal{A}/2). \quad (19)$$

This has to be contrasted with the full result coming from (17)

$$\mathcal{W}_1 = \exp \left[ -\frac{g^2 N \mathcal{A}}{4} \right], \quad (20)$$

giving the expected area-law exponentiation, that can be easily derived directly on the plane by resumming the perturbative series in which the light-cone propagator is *CPV*-prescribed according to 't Hooft [12]. Actually, in the large- $N$  limit, (19) does not exhibit confinement, as first noticed in [21]. As a matter of fact from (19), taking the limit  $N \rightarrow \infty$  ( $\hat{g}^2 = g^2 N$ ),

$$\lim_{N \rightarrow \infty} \mathcal{W}_1^{(0)} = \sqrt{\frac{2}{\hat{g}^2 \mathcal{A}}} J_1 \left( \sqrt{2\hat{g}^2 \mathcal{A}} \right); \quad (21)$$

however, this is hardly surprising since  $\mathcal{W}_1^{(0)}$  does not contain any genuine non-perturbative contribution, and simply reproduces the Wilson loop behaviour of the weak-coupling phase of the sphere [24], where instantons are suppressed [25,26,22].

For a general winding  $n$ , Eq. (17) is therefore expected to come out from the resummation of 't Hooft perturbative series, that corresponds to a light-front quantization of the theory [5]. On the other hand to neglect instantons, and then to send the area of the sphere to infinity, is likely to reproduce the WML computation: the perturbative analysis will confirm these claims. At the moment we need the zero instanton contribution to (17): it can be easily obtained, closely following ref. [13], by applying a Poisson resummation to (6) and taking the non-exponentially suppressed terms as  $g^2 \rightarrow 0$

$$\mathcal{W}_n^{(0)} = \frac{1}{N} \exp \left[ -g^2 \frac{(A - \mathcal{A})\mathcal{A}}{4A} n^2 \right] L_{N-1}^{(1)} \left( g^2 \frac{(A - \mathcal{A})\mathcal{A}}{2A} n^2 \right). \quad (22)$$

For  $A \rightarrow \infty$  it becomes

$$\mathcal{W}_n^{(0)} = \frac{1}{N} \exp \left[ -\frac{g^2 \mathcal{A} n^2}{4} \right] L_{N-1}^{(1)} (g^2 \mathcal{A} n^2 / 2). \quad (23)$$

The above result is quite different from (17) and reflects much more dramatically the same discrepancy found for  $n = 1$ : the string tension is independent from  $N$  and there is no trace of the non-abelian nature, since different exponential weights do not appear. Actually, the behaviour of  $\mathcal{W}_n^{(0)}$  (the WML one) is, with respect to the fundamental winding  $n = 1$ , *exactly* the same as in the abelian  $U(1)$  theory. It is easily proved for  $U(1)$  that

$$\mathcal{W}_n(\mathcal{A}; 1) = \exp \left[ -\frac{g^2 \mathcal{A} n^2}{4} \right], \quad (24)$$

the  $n$  windings resulting trivially in replacing the charge  $g$  by  $gn$ . The WML result satisfies the same rule as it is clearly seen from (23)

$$\mathcal{W}_n^{(0)}(g^2 \mathcal{A}; N) = \mathcal{W}_1^{(0)}(g^2 n^2 \mathcal{A}; N). \quad (25)$$

In this perspective the exact (*i.e.* full instantons 't Hooft) result does not seem related to any simple-minded reduction  $U(N) \sim U(1)^N$ , suggested by the abelianization of the theory in axial gauges; rather a non-trivial (non-abelian) effect is present there.

We can further observe another basic difference between Eq. (17) and Eq. (23): as a matter of fact, the former shows an interesting symmetry between  $N$  and  $n$ . More precisely, we have that

$$\begin{aligned} \mathcal{W}_n(\mathcal{A}; N) &= \mathcal{W}_N(\tilde{\mathcal{A}}; n) \\ \tilde{\mathcal{A}} &= \frac{n}{N} \mathcal{A}, \end{aligned} \quad (26)$$

a relation that is far from being trivial, involving an unexpected interplay between the geometrical and the algebraic structure of the theory. Looking at Eq. (26), the abelian-like exponentiation for  $U(N)$  when  $n = 1$  appears to be connected to the  $U(1)$  loop with  $N$

windings, the “genuine” triviality of Maxwell theory providing the expected behaviour for the string tension. Moreover we notice the intriguing feature that the large- $N$  limit (with  $n$  fixed) is equivalent to the limit in which an infinite number of windings is considered with vanishing rescaled loop area. Alternatively, this rescaling could be thought to affect the coupling constant  $g^2 \rightarrow \frac{n}{N}g^2$ . Eq. (23), of course, does not exhibit such a fancy behaviour; nevertheless it is related, in a particular dynamical limit, to the full result, as we will see in the following.

Let us discuss in detail the large- $N$  limit of Eq. (17): it was obtained long ago by Kazakov and Kostov [17]<sup>2</sup>, who solved the Makeenko-Migdal equations in the case at hand. Coming back to Eq. (15), we introduce the function  $\hat{\mathcal{W}}_n(\mathcal{A}; N)$  from

$$\mathcal{W}_n(\mathcal{A}; N) = \exp\left[-\frac{g^2 \mathcal{A} N n}{4}\right] \hat{\mathcal{W}}_n(\mathcal{A}; N),$$

that can be expressed through a contour integral

$$\begin{aligned} \hat{\mathcal{W}}_n(\mathcal{A}; N) &= -\frac{1}{Nn} \sum_{k=0}^{n-1} \exp\left[\frac{g^2 \mathcal{A}}{2} n \left(k - \frac{n-1}{2}\right)\right] \frac{(-1)^k}{k!} \\ &\times \frac{n!}{(n-1-k)!} \frac{1}{2\pi i} \oint_C dt t^{k-n} (1-t)^{n-1} \end{aligned} \quad (27)$$

( $C$  is a contour surrounding the origin of the complex plane). The binomial sum can be performed and, after reversing the path around the pole at  $t = 1$  and finally changing variable ( $z = 1 + t$ ), we get

$$\hat{\mathcal{W}}_n(\mathcal{A}; N) = \frac{(-1)^n}{2\pi i N} \exp\left[-g^2 \mathcal{A} \frac{n(n-1)}{4}\right] \oint_C \frac{dz}{(1+z)^N} \frac{[1 - (1+z) \exp(g^2 \mathcal{A} n/2)]^{n-1}}{z^{n+1}}. \quad (28)$$

The case  $n \geq N$  is easily obtained from Eq. (17) by exploiting the symmetry between  $n$  and  $N$  (Eq. (26)).

---

<sup>2</sup>The explicit form for finite  $N$  and small  $n$  ( $n = 2, 3$ ) can be deduced from [17] and [18]. The latter used a non-abelian version of Stokes’ theorem, and both are consistent with our general formula (17).

Eq. (28) is a nice representation for the Wilson loop with  $n$  windings, which is particularly suitable to discuss the large- $N$  limit. Actually, rescaling  $z$  into  $\frac{z}{N}$ , we have

$$\hat{\mathcal{W}}_n(\mathcal{A}; N) = \frac{(-1)^n}{2\pi i} \exp \left[ -g^2 \mathcal{A} \frac{n(n-1)}{4} \right] \oint_C \frac{dz}{(1 + \frac{z}{N})^N} \frac{[N - (N+z) \exp(g^2 \mathcal{A} n/2)]^{n-1}}{z^{n+1}}, \quad (29)$$

and then, by taking the limit  $N \rightarrow \infty$ ,  $\hat{g}^2 = g^2 N$  fixed, we arrive at

$$\begin{aligned} \hat{\mathcal{W}}_n(\mathcal{A}; N) &= -\frac{2}{\hat{g}^2 \mathcal{A} n} \frac{1}{2\pi i} \oint_C dx \frac{(1+x)^{n-1}}{x^{n+1}} \exp \left[ -\frac{\hat{g}^2 \mathcal{A} n x}{2} \right] \\ &= -\frac{2}{\hat{g}^2 \mathcal{A} n} L_{n-1}^{(-1)}(\hat{g}^2 \mathcal{A} n/2), \end{aligned} \quad (30)$$

from which we can easily recover the Kazakov-Kostov result

$$\mathcal{W}_n(\mathcal{A}; \infty) = \frac{1}{n} L_{n-1}^{(1)}(\hat{g}^2 \mathcal{A} n/2) \exp \left[ -\frac{\hat{g}^2 \mathcal{A} n}{4} \right]. \quad (31)$$

Using Eq. (26) we are able to perform another limit, namely  $n \rightarrow \infty$  with fixed  $n^2 \mathcal{A}$

$$\lim_{n \rightarrow \infty} \mathcal{W}_n(\mathcal{A}; N) = \frac{1}{N} L_{N-1}^{(1)}(g^2 \mathcal{A} n^2/2) \exp \left[ -\frac{g^2 \mathcal{A} n^2}{4} \right]. \quad (32)$$

Eq. (32) *exactly* coincides with the WML result Eq. (23): this means that in the small area limit (taking  $n \rightarrow \infty$  in order to have a non-vanishing interaction) we essentially recover the zero-instanton, *i.e.* perturbative, approximation, even from the exact formula Eq. (17). The same behaviour will show up when studying the spectral density for Wilson loop eigenvalues (see Sect. IV). Once again the reason for the equivalence of Eqs. (32) and (23) is founded on the non-trivial geometrical aspects encoded in Eq. (17). In fact, we recall that in Eq. (23) we have neglected the instanton contributions: we expect that sufficiently small loops are unaffected by instantons due to their having a typical length scale measured by their size. Eq. (32) supports this intuitive argument.

This conclusion is not limited to the decompactified case: we can go further and prove that, even at finite total area  $A$ , the exact heat-kernel expression Eq. (6) reduces to Eq. (22) when  $n \rightarrow \infty$ <sup>3</sup>. Introducing  $\lambda = n^2 \mathcal{A}$ , we can write Eq. (6) as

---

<sup>3</sup>We need to have  $n \rightarrow \infty$  with  $n^2 \mathcal{A}$  fixed so that the interaction is finite.

$$\begin{aligned} \mathcal{W}_n \mathcal{Z} &= \exp \left[ -\frac{g^2 A}{48} N(N^2 - 1) \right] \exp \left[ -\frac{g^2 \lambda}{4} \right] \sum_{m_i = -\infty}^{\infty} \exp \left[ -\frac{g^2 A}{4} \sum_{i=1}^N m_i^2 - \frac{g^2 \lambda}{2} \frac{m_1}{n} \right] \\ &\times \Delta^2(m_1, \dots, m_N) \prod_{j=2}^N \left( 1 + \frac{n}{m_1 - m_j} \right). \end{aligned}$$

Expanding the product we get

$$\begin{aligned} \mathcal{W}_n \mathcal{Z} &= \exp \left[ -\frac{g^2 A}{48} N(N^2 - 1) \right] \exp \left[ -\frac{g^2 \lambda}{4} \right] \sum_{k=0}^{N-1} \frac{(N-1)!}{(N-1-k)!} n^k \\ &\times \sum_{\hat{m}_i} \exp \left[ -\frac{g^2 A}{4} \sum_{i=1}^N m_i^2 - \frac{g^2 \lambda}{2} \frac{m_1}{n} \right] \Delta^2(m_1, \dots, m_N) \prod_{j=2}^{k+1} \frac{1}{m_1 - m_j}. \end{aligned}$$

We obtain a series in  $1/n$  from the expansion of the exponential term

$$\begin{aligned} \mathcal{W}_n \mathcal{Z} &= \exp \left[ -\frac{g^2 A}{48} N(N^2 - 1) \right] \exp \left[ -\frac{g^2 \lambda}{4} \right] \sum_{l=0}^{\infty} \sum_{k=0}^{N-1} \frac{(N-1)!}{(N-1-k)!} n^{k-l} \frac{(-g^2 \lambda)^l}{2^l l!} \\ &\times \sum_{m_i = -\infty}^{\infty} \exp \left[ -\frac{g^2 A}{4} \sum_{i=1}^N m_i^2 \right] \Delta^2(m_1, \dots, m_N) \prod_{j=2}^{k+1} \frac{m_1^l}{m_1 - m_j}. \end{aligned} \quad (33)$$

Eq. (33) is truly an expansion in  $1/n^2$ : in order to understand this point, we simply notice that changing  $m_i \rightarrow -m_i$  we produce an overall factor  $(-1)^{k+l}$  weighting the sum over  $m_i$ . This implies that  $k+l$  (and therefore  $k-l$ ) must be an even integer so as to have a non-vanishing result. It is useful to rewrite the sum over  $m_i$  as

$$\frac{1}{(k+1)!} \sum_{m_i = -\infty}^{\infty} \exp \left[ -\frac{g^2 A}{4} \sum_{i=1}^N m_i^2 \right] \Delta^2(m_1, \dots, m_N) \sum_P \prod_{j=2}^{k+1} \frac{m_{P(1)}^l}{m_{P(1)} - m_{P(j)}},$$

where the sum over  $P$  is over the elements of the permutation group  $S_{k+1}$ . Let us evaluate to the 0<sup>th</sup>-order term: we observe that for  $l = k$

$$\sum_P \prod_{j=2}^{k+1} \frac{m_{P(1)}^l}{m_{P(1)} - m_{P(j)}} = \frac{1}{\Delta(m_1, \dots, m_{k+1})} \sum_P f_P(m_1, \dots, m_{k+1}), \quad (34)$$

the Vandermonde determinant being produced by the common denominator; the quantity  $\sum_P f_P(m_1, \dots, m_{k+1})$  is a polynomial of degree  $\frac{k(k+1)}{2}$  in  $k+1$  variables. Since the Vandermonde determinant  $\Delta(m_1, \dots, m_{k+1})$  is totally antisymmetric, the non-vanishing contribution to Eq. (33) comes from the totally antisymmetric part of  $\sum_P f_P(m_1, \dots, m_{k+1})$ , implying that

$$\sum_P f_P(m_1, \dots, m_{k+1}) \simeq c \Delta(m_1, \dots, m_{k+1}).$$

The constant  $c$  is easily proven to be 1 by inspection of Eq. (34). Hence the contribution of order  $(\frac{1}{n^2})^0$  to Eq. (33) is

$$\begin{aligned} \mathcal{W}_n \mathcal{Z} &= \exp \left[ -\frac{g^2 A}{48} N(N^2 - 1) \right] \left[ \sum_{k=0}^{N-1} \frac{(N-1)!}{(N-1-k)!} \frac{(-1)^k}{k!(k+1)!} \left( \frac{g^2 \lambda}{2} \right)^k \right] \\ &\times \sum_{m_i=-\infty}^{\infty} \exp \left[ -\frac{g^2 A}{4} \sum_{i=1}^N m_i^2 \right] \Delta^2(m_1, \dots, m_N) \\ &= \mathcal{Z}[A] \frac{1}{N} L_{N-1}^{(1)}(g^2 \lambda/2) e^{-\frac{g^2 \lambda}{4}}, \end{aligned} \quad (35)$$

proving that the 0<sup>th</sup>-order contribution is exactly the WML one. It remains to show that the divergent contributions (coming from  $l < k$  in Eq. (33)) are vanishing. To this purpose we use again Eq. (34) to notice that we can still factorize a Vandermonde determinant in the denominator, but now  $\sum_P f_P(m_1, \dots, m_{k+1})$  is a polynomial of degree less than  $\frac{k(k+1)}{2}$  in  $k+1$  variables. Its totally antisymmetric part vanishes, so that

$$\lim_{\substack{n \rightarrow \infty \\ \lambda \text{ fixed}}} \mathcal{W}_n(A - \mathcal{A}, \mathcal{A}) \sim \frac{1}{N} L_{N-1}^{(1)}(g^2 \lambda/2) \exp \left[ -\frac{g^2 \lambda}{4} \right] + \mathcal{O} \left( \frac{1}{n^2} \right).$$

This confirms our guess that sufficiently small loops do not see instantons: actually it is known that in the strong phase (at large- $N$ ) small loops behave as in the weak phase (*i.e.* they do not confine) as  $n \rightarrow \infty$ . Our result goes further, revealing that even at finite  $N$  and at finite total area  $A$ , instantons can be dynamically suppressed.

### III. THE PERTURBATIVE WML AND 'T HOOFT PRESCRIPTIONS

We now turn to the resummation of the perturbative expansion for  $\mathcal{W}_n$ . The aim of our investigation is not only to check the correctness of the interpretation of the non-perturbative results derived so far, but more importantly to observe and explain a curious interplay between geometry and colour factors in the two different prescriptions. We will begin with WML, for which the resummation of the perturbative series is found through a simple generalization of the procedure outlined in [21] in the case  $n = 1$ . This is due to all diagrams entailing the same geometrical factor. We will then switch to 't Hooft prescription and realize



the resummation is rather involved since graphs belonging to the same class, according to their colour factor, produce different geometrical integrals. Hence, in this respect, light-front quantization exhibits its peculiar non-abelian character.

### A. Resummation of the perturbative series defined via WML prescription

We closely follow the procedure outlined in [21]. In the euclidean space the perturbative expansion of  $\mathcal{W}_n$  is

$$\mathcal{W}_n[\mathcal{A}] = 1 + \frac{1}{N} \sum_{k=1}^{\infty} (-g^2)^k \int_0^1 ds_1 \dot{x}^{\mu_1}(s_1) \cdots \int_0^{s_{2k-1}} ds_{2k} \dot{x}^{\mu_{2k}}(s_{2k}) \text{Tr} [G_{\mu_1 \cdots \mu_{2k}}(x_1, \cdots, x_{2k})], \quad (36)$$

where  $x^\mu(s)$ ,  $s \in [0, 1]$  parametrizes the contour with  $n$  windings. The Lie algebra-valued  $2k$ -point Green function  $G_{\mu_1 \cdots \mu_{2k}}(x_1, \cdots, x_{2k})$  has to be expressed via the Wick rule in terms of the free propagator  $D(x_i - x_j)$ , in the light cone gauge  $A_- = 0$  and endowed with (Wick-rotated) WML prescription

$$D_{++}^{ab}(x - x') = \frac{1}{2\pi} \delta^{ab} \frac{x_+ - x'_+}{x_- - x'_-}. \quad (37)$$

The simplest choice for the contour is a circle wrapping around itself  $n$  times. Then it happens [21] that the weighted basic correlator is independent of the loop variables, since

$$\dot{x}_-(s) \dot{x}_-(s') \frac{x_+(s) - x_+(s')}{x_-(s) - x'_-(s')} = 2(n\pi r)^2.$$

After that, the integration over the path parameters  $s_1, \cdots, s_{2k}$  trivially yields  $1/(2k)!$  and the task of determining the Wilson loop reduces to the purely combinatorial problem of finding the group factors corresponding to the Wick contractions. What is left is

$$\mathcal{W}_n[\mathcal{A}] = 1 + \frac{1}{N} \sum_{k=1}^{\infty} \left( -\frac{g^2 n^2 \mathcal{A}}{2} \right)^k \frac{c_{2k}(N)}{(2k)!},$$

where  $c_{2k}(N)$  is the sum over all possible traces of  $2k$   $T^a$  matrices suitably contracted. Fortunately this group factor is generated by a matrix integral [21], and the final result reads

$$\mathcal{W}_n[\mathcal{A}] = \frac{1}{N} \exp \left[ -\frac{1}{4} g^2 n^2 \mathcal{A} \right] L_{N-1}^{(1)}(g^2 n^2 \mathcal{A}/2), \quad (38)$$

reproducing the zero-instanton result Eq. (23) obtained via non-perturbative methods.

### B. Resummation of the perturbative series defined via 't Hooft prescription

As already hinted, we were not able to resum the full perturbative expansion for  $\mathcal{W}_n$  prescribed with 't Hooft. We believe after exertion that such a formidable task is, if not impossible, at least extremely tough. Nevertheless we were successful in the computation of the Wilson loop with  $n$  windings at  $\mathcal{O}(g^4)$ , which suffices to give a flavour on how things work at higher orders. Moreover we performed the limit  $n \rightarrow \infty$ ,  $n^2 \mathcal{A}$  fixed, and, by exploiting the duality  $n \leftrightarrow N$ , the large- $N$  limit, with  $g^2 N$  fixed.

Firstly, let us start from the perturbative definition of  $\mathcal{W}_n$  in the light-cone gauge ( $A_- = 0$ )

$$\mathcal{W}_n = \frac{1}{N} \mathcal{N} \text{Tr} \left\{ \int \mathcal{D}A_\mu \exp \left[ i \int d^2x \left( -\frac{1}{4} F_{\mu\nu}^a F^{\mu\nu a} + J_\mu^a A^{\mu a} \right) \right] \delta(A_-^a) \mathcal{P} \exp \left( i g \oint_n A_\mu^a T^a dx^\mu \right) \right\}, \quad (39)$$

evaluated at  $J^a = 0$ . It is easy to recognize that Eq. (39) can be rewritten as follows

$$\mathcal{W}_n = \frac{1}{N} \mathcal{N} \text{Tr} \left\{ \mathcal{P} \exp \left[ g \oint_n T^a \frac{\delta}{\delta J^a(x)} dx^+ \right] \exp \left[ -\frac{1}{2} \int d^2x d^2y J^a(x) D(x-y) J^a(y) \right] \right\}_{J=0}, \quad (40)$$

where now the propagator  $D(x-y)$  is defined through the CPV prescription Eq. (2). We consider a light-like rectangle with sides  $2L$ ,  $2T$  (see Fig. 1) and choose the currents with support on the contour, so that

$$J^a(x^+, x^-) = j_u^a \delta(x^- - L) + j_d^a \delta(x^- + L).$$

With this choice the perturbative expansion Eq. (40) for  $\mathcal{W}_n$  reads

$$\begin{aligned}
\mathcal{W}_n = \frac{1}{N} \mathcal{N} \text{Tr} \left\{ \mathcal{P} \exp \left[ g \oint_{C_{2,n}} T^{a_n} j_d^c \frac{\delta}{\delta j_u^{a_n}(x^+)} dx^+ \right] \mathcal{P} \exp \left[ g \oint_{C_{1,n}} T^{b_n} \frac{\delta}{\delta j_d^{b_n}(x^+)} dx^+ \right] \right. \\
\left. \cdots \mathcal{P} \exp \left[ g \oint_{C_{2,1}} T^{a_1} \frac{\delta}{\delta j_u^{a_1}(x^+)} dx^+ \right] \mathcal{P} \exp \left[ g \oint_{C_{1,1}} T^{b_1} \frac{\delta}{\delta j_d^{b_1}(x^+)} dx^+ \right] \right. \\
\left. \exp \left[ iL \int_{-T}^T dx^+ j_u^c(x^+) j_d^c(x^+) \right] \right\}_{j=0} \quad (41)
\end{aligned}$$

with  $C_1$  and  $C_2$  as in Fig. 1. Clearly in the limit  $j_u^a, j_d^a \rightarrow 0$  the only non-vanishing contributions are those with a matching number of derivatives with respect to  $j_u$  and  $j_d$ .

Now everything is settled and we can easily derive the expression of  $\mathcal{W}_n^{(4)}$ , *i.e.* the Wilson loop with  $n$  windings  $\mathcal{O}(g^4)$ . The following prefactor is common to all classes of diagrams

$$g^4 (iL)^2 (2T)^2 = -\frac{g^4 \mathcal{A}^2}{4}, \quad (42)$$

$\mathcal{A} = 4LT$  being the area of the loop. As a matter of fact,  $g^4$  comes from four derivatives with respect to the currents which contribute at this order,  $(iL)^2$  is produced when two derivatives act on the last exponential in Eq. (41), which represents the only non-vanishing contribution, and finally  $(2T)^2$  is given by integration over the loop variables. Notice the expected dependence on the area due to invariance with respect to area-preserving diffeomorphisms typical of  $d = 2$ .

In Appendix A we show which classes of non-crossed and crossed diagrams contribute to  $\mathcal{W}_n^{(4)}$  and also provide the exact counting (as a function of  $n$ ) and area factor. The latter turns out to be either  $\frac{1}{2}$  or 1 depending on the presence of integrals in the loop variables which are nested as a consequence of the definition of the  $\mathcal{P}$  exponential. Furthermore one has to take into account that non-crossed diagrams produce an additional factor  $N^3/4$  from  $\text{Tr} [T^a T^a T^b T^b]$ , whereas the analog for crossed diagrams is  $N/4$  from  $\text{Tr} [T^a T^b T^a T^b]$ . Remember eventually the factor  $1/N$  appearing in Eq. (41).

We present here the final results, which read

$$\mathcal{W}_n^{(4), nc} = -\frac{g^4 \mathcal{A}^2 n^2}{96} N^2 (2n^2 + 1) \quad (43)$$

$$\mathcal{W}_n^{(4), c} = -\frac{g^4 \mathcal{A}^2 n^2}{96} (n^2 - 1) \quad (44)$$

and, summing up,

$$\mathcal{W}_n^{(4)} = -\frac{g^4 \mathcal{A}^2 n^2}{96} (2n^2 N^2 + N^2 + n^2 - 1) , \quad (45)$$

which coincides with the coefficient  $\mathcal{O}(g^4)$  of the expansion of Eq. (17) obtained via non-perturbative methods. Moreover, already at this level, the symmetry under the exchange  $n \leftrightarrow N$  is manifest once the area is rescaled by  $N/n$ .

Let us now go back to Eq. (41) in order to extrapolate the relevant limits  $n \rightarrow \infty$  and  $N \rightarrow \infty$ . We have already stressed that they are dual to each other (provided the loop area is suitably rescaled), so that we will explicitly perform only the former and deduce the latter by symmetry. In Sect. II the large- $n$  limit of the non-perturbative  $\mathcal{W}_n$ , with  $\mathcal{A}n^2$  fixed, was proved to coincide with the resummation of the perturbative series when WML prescription was adopted and  $\mathcal{A} \rightarrow \mathcal{A}n^2$ . Thus we guess that at large  $n$  dominant configurations of loop diagrams where 't Hooft prescription is imposed must be weighted by the same area factor. This precisely happens for WML as we realized in Sect. IIIA. In fact, by inspecting the computation of  $\mathcal{W}_n$  at order  $\mathcal{O}(g^4)$  we are easily convinced that in this limit dominant configurations, either crossed or non-crossed, are those which spread through the maximum number of sheets of the  $n$ -fold loop, *i.e.* those in which the vector fields are all attached on different sides of the loop. For instance the leading terms at  $\mathcal{O}(g^4)$  are those shown in Figs. 1i, 2d. Going further, at a generic order  $g^{2k}$  one needs at least  $2k$  sheets in order to set up such configurations, and their number is straightforwardly determined. Actually, there are  $\binom{n}{2k}$  ways of extracting  $2k$  sheets out of  $n$  and in addition we have to take into account all possible configurations of the basic  $2k$ -sheet structure with any kind of cross-over. Therefore, the counting of dominant configurations is given by

$$\frac{n!}{(2k)! (n-2k)!} \times c_{2k}(N) , \quad (46)$$

where  $c_{2k}(N)$  is the coefficient we acquainted with in Sect. IIIA. Hence, at the leading order in  $n$ , we end up with

$$W_{n \rightarrow \infty}(\mathcal{A}) = \frac{1}{N} \sum_{k=0}^{\infty} \left( -\frac{g^2 \mathcal{A} n^2}{2} \right)^k \frac{c_{2k}(N)}{(2k)!} \quad (47)$$

and, switching to the euclidean space via a Wick rotation

$$W_{n \rightarrow \infty}(\mathcal{A}) = \frac{1}{N} \exp \left[ -\frac{1}{4} g^2 \mathcal{A} n^2 \right] L_{N-1}^{(1)} \left( \frac{g^2 \mathcal{A} n^2}{2} \right), \quad (48)$$

which corresponds to Eq. (23).

The next step consists in performing the large- $N$  limit of the resummed perturbative series in the axial gauge with the light-cone CPV prescription. The duality  $n \leftrightarrow N$  allows us to conclude

$$W_{N \rightarrow \infty}(\mathcal{A}) = \frac{1}{n} \exp \left[ -\frac{1}{4} \hat{g}^2 \mathcal{A} n \right] L_{n-1}^{(1)} \left( \frac{\hat{g}^2 \mathcal{A} n}{2} \right), \quad (49)$$

where the rescaling in Eq. (26) is understood. Apart from the numerical coincidence, the duality entails a deep relation among different faces of the same theory. Naively one could think that the large- $N$  limit, being dominated by non-crossed graphs in which the trace factor considerably simplifies, is easy to recover. Nevertheless, a surprising complexity in the integrals over loop variables arises, since every class of diagrams is characterized by a different area factor. This is already manifest from the computation of the Wilson loop at order  $g^4$  (see Appendix A). Thus the most relevant conclusion we can draw is that an enlightening interplay between geometry and algebraic invariants takes place, connecting the large- $N$  with the large- $n$  limit and, in a sense, the strong and the weak phase of the theory.

#### IV. THE SPECTRAL DENSITY

$U(N)$  Yang-Mills theory on the sphere  $S^2$  exhibits in the large- $N$  limit with  $g^2 N$  fixed, a third order phase transition (Douglas-Kazakov (DK) phase transition) [24]. According to the total area  $A$  of the sphere, two different regimes occur: a strong coupling regime when  $A > \pi^2$  (in suitable units, *i.e.*  $\frac{g^2 N}{2} = 1$ ) and a weak coupling regime with  $A < \pi^2$ . The difference between them can be traced back to the presence of instantons on the sphere [25,26,22], which fully contribute for large  $A$ , but are instead exponentially suppressed in the weak-coupling phase.

The two regimes can be conveniently characterized by the density  $\rho$  of Young tableaux indices which single out the various irreducible representations of the group  $U(N)$ . In the strong coupling regime the distribution  $\rho$  undergoes a phenomenon of “saturation” in the large- $N$  limit, namely it is equal to one in a finite interval of its domain. In turn, if we consider a Wilson loop on the sphere with the contour  $C$  running around an equator and winding an arbitrary number  $n$  of times, the density  $\rho$  is related by a kind of duality transformation [22] to the spectral density  $\sigma$  on the unit circle of the eigenvalues of the unitary operator  $U_C$ , representing the loop.

The strong-coupling phase is characterized by the fact that those eigenvalues completely fill the unit circle, whereas in the weak coupling regime a gap develops where the distribution  $\sigma$  vanishes. Before decompactifying the sphere to the plane by taking the limit  $A \rightarrow \infty$ , we have to learn how the density  $\sigma$  evolves when we replace the equatorial contour with a smooth arbitrary one. In ref. [22] it is shown that, when one of the two different areas generated in this way, let us call it  $\mathcal{A}$ , becomes small enough, a gap in the eigenvalue distribution appears even in the strong DK phase (*i.e.* for  $A > \pi^2$ ). Actually, when the total area  $A$  approaches its critical value  $\pi^2$  from above,  $\mathcal{A}$  becomes critical at its maximum value  $\mathcal{A}_{cr} = \frac{\pi^2}{2}$ , namely when the contour is along an equator.

When the sphere is decompactified to the plane by taking the limit  $A \rightarrow \infty$  at fixed  $\mathcal{A}$ , we are automatically in the DK strong phase; it is then remarkable that  $\mathcal{A}_{cr}$  reaches, in the limit  $A \rightarrow \infty$ , a well defined value,  $\mathcal{A}_{cr} = 4$ .

We are going to obtain all these results from the explicit expressions we got in Sect. II for Wilson loops with an arbitrary winding number  $\mathcal{W}_n$ . We shall explicitly discuss the large- $N$  case on the plane ( $A \rightarrow \infty$ ). The spectral density  $\sigma(\mathcal{A}, \theta)$ ,  $\mathcal{A}$  being the area enclosed by the loop, is related to  $\mathcal{W}_n$  by the following Fourier series [14]

$$\sigma(\mathcal{A}, \theta) = \frac{1}{2\pi} \left[ 1 + 2 \sum_{n=1}^{\infty} \cos(n\theta) \mathcal{W}_n \right]. \quad (50)$$

We shall compute this function and show that, according to different values of  $\mathcal{A}$ , a gap may develop in the  $\theta$ -variable in which the distribution vanishes. This phenomenon was

first noticed by Durhuus and Olesen [16], who derived the spectral function solving a kind of Makeenko-Migdal equation with suitable boundary conditions.

By introducing Eq. (31) into Eq. (50) we get

$$\sigma(\mathcal{A}, \theta) = \frac{1}{2\pi} \left[ 1 + \sum_{n=1}^{\infty} (e^{in\theta} + e^{-in\theta}) \frac{1}{n} e^{-\frac{n\mathcal{A}}{2}} L_{n-1}^{(1)}(n\mathcal{A}) \right] = \frac{1}{2\pi} [1 + 2\text{Re} F(\mathcal{A}, \theta)] , \quad (51)$$

where

$$F(\mathcal{A}, \theta) = \sum_{n=1}^{\infty} \frac{1}{n} e^{-n(\frac{\mathcal{A}}{2} - i\theta)} \oint_{\Gamma} \frac{dt}{2\pi i} e^{-nAt} \left( 1 + \frac{1}{t} \right)^n . \quad (52)$$

Here we have used a well-known integral representation for the Laguerre polynomials in which the integration contour  $\Gamma$  encircles the origin of the complex  $t$ -plane.

When the inequality

$$\left| e^{-\mathcal{A}(t+\frac{1}{2})} \left( 1 + \frac{1}{t} \right) \right| < 1 \quad (53)$$

is satisfied, the series in Eq. (52) can be summed giving rise to a *single-valued* function

$$\sum_{n=1}^{\infty} \frac{1}{n} e^{-n[\mathcal{A}(t+\frac{1}{2}) - i\theta]} \left( 1 + \frac{1}{t} \right)^n = -\log \left[ 1 - e^{-\mathcal{A}(t+\frac{1}{2}) + i\theta} \left( 1 + \frac{1}{t} \right) \right] . \quad (54)$$

The logarithm in turn can be analytically continued; as is well known, it has branch points when its argument either vanishes or diverges. Whereas it is easy to realize that the only divergence occurs, at finite  $|t|$ , at  $t = 0$ , a careful study of the roots of the transcendental equation

$$e^{-\mathcal{A}(t+\frac{1}{2}) + i\theta} \left( 1 + \frac{1}{t} \right) = 1 \quad (55)$$

is in order before drawing any conclusion.

It is amusing to notice that the change of variable

$$t = \frac{\exp(i\xi)}{1 - \exp(i\xi)} \quad (56)$$

turns Eq. (55) into Eq.(3.4) of ref. [16].

To the success of our calculation it is essential that the contour  $\Gamma$  in Eq. (52) can be deformed while the logarithm still remaining single-valued on it.

The discussion of the roots of Eq. (55) is deferred to Appendix B. There we show that, for  $\mathcal{A} > 4$ , only two roots are possible and only one of them is encircled by the contour  $\Gamma$ . If we set  $t = x + iy$  and denote this root by the values  $(\hat{x}, \hat{y})$ , which obviously are functions of  $\mathcal{A}$  and of  $\theta$ , a cut can be drawn along the segment  $(0, 0) - (\hat{x}, \hat{y})$  in the complex  $t$ -plane and the contour  $\Gamma$  can be deformed to the contour  $\gamma$ , encircling the branch points and just running below and above the cut. It is then immediate to conclude that

$$F(\mathcal{A}, \theta) = \hat{x} + i\hat{y}$$

and that, eventually,

$$\sigma(\mathcal{A}, \theta) = \frac{1}{\pi} \left( \hat{x} + \frac{1}{2} \right). \quad (57)$$

As long as  $\mathcal{A} > 4$ ,  $\hat{x} + \frac{1}{2}$  is positive for any value of  $\theta$ . The eigenvalues are filling the entire interval  $(-\pi, \pi)$ .

When  $\mathcal{A} < 4$  the situation dramatically changes. Although we are in the strong DK phase (we are on the plane), a gap starts showing up in the eigenvalue density for  $\theta$  close to  $\pi$  (and to  $-\pi$ ; remember  $\sigma$  is an even function of  $\theta$ ). Actually, for  $\mathcal{A} < 4$ , there is a value  $\theta_{cr} < \pi$  such that  $\hat{x}(\mathcal{A}, \theta_{cr}) = -\frac{1}{2}$ . Once this value of  $\theta$  is reached,  $\hat{x}$  remains equal to  $-\frac{1}{2}$ , and consequently  $\sigma$  vanishes.

In Appendix B we show that the expression for  $\theta_{cr}$  coincides with the one in Eq.(4.8) of ref. [16], namely

$$\theta_{cr} = \sqrt{\mathcal{A} - \frac{\mathcal{A}^2}{4}} + \arccos \left( 1 - \frac{\mathcal{A}}{2} \right). \quad (58)$$

Eventually, in the limit  $\mathcal{A} \rightarrow 0$ , the density approaches the periodic  $\delta$ -distribution, as it should.

Actually we have already seen in Sect. II that, in the small- $\mathcal{A}$  limit, instantons on the sphere are suppressed even in the strong DK phase. This phenomenon has a simple geometrical interpretation: it occurs when one of the two areas singled out by the loop gets small when compared to the instanton size. It might then seem that the different behaviour of



$\sigma$  according to the values of  $\mathcal{A}$ , is fully driven and characterized by instantons. This issue would in turn be of crucial relevance in singling out peculiar properties of the light-front vacuum when compared to the one in equal-time canonical Fock space after decompactification of the sphere to the plane.

Unfortunately the situation is not as simple as that. In ref. [13] the contribution to the Wilson loop from the zero-instanton sector on  $S^2$  was clearly pointed out. It was also noticed that, in the decompactification limit, this contribution exactly coincides with the sum of the perturbative series when graphs are evaluated according to the WML prescription for the propagator. In Sect. II we have generalized this result to a loop with an arbitrary winding number  $n$ . It is then a fairly simple exercise to take the large- $N$  limit and to insert the result in Eq. (50)

$$\sigma^{ML} = \frac{1}{2\pi} \left[ 1 + 2 \sum_{n=1}^{\infty} \frac{\cos(n\theta)}{n\sqrt{\mathcal{A}}} J_1(2n\sqrt{\mathcal{A}}) \right], \quad -\pi \leq \theta \leq \pi, \quad (59)$$

$J_1$  being the usual Bessel function. Of course its geometrical meaning is now completely different.

Still, due to the absence of instantons, one would naively believe that  $\sigma^{ML}$  should behave like in a weak phase, in particular should develop a gap. But this is not always the case; as a matter of fact, using a standard integral representation for the Bessel function, we get

$$\sigma^{ML} = \frac{2}{\pi} \int_{-1}^1 dt \sqrt{1-t^2} \delta_P(\theta + 2t\sqrt{\mathcal{A}}), \quad (60)$$

$\delta_P$  being the periodic  $\delta$ -distribution, leading to

$$\sigma^{ML} = \frac{1}{\pi\sqrt{\mathcal{A}}} \sum_m \sqrt{1 - \frac{(2\pi m + \theta)^2}{4\mathcal{A}}}, \quad -\pi \leq \theta \leq \pi, \quad (61)$$

the sum running over all positive and negative values of  $m$  such that the argument of the square root is positive.

It is easy to check that this expression reproduces the limits

$$\lim_{\mathcal{A} \rightarrow \infty} \sigma^{ML} = \frac{1}{2\pi}$$

and

$$\lim_{\mathcal{A} \rightarrow 0} \sigma^{ML} = \delta(\theta).$$

For  $\mathcal{A} < \frac{\pi^2}{4}$  there is indeed a gap, similar to the one in the weak phase on the sphere, but with a new threshold. For larger values the gap disappears.

Only the functional form (a square root) is reminiscent of a weak phase. There are moreover discontinuities in the derivative of the density anytime a new value of  $m$  starts contributing.

One would eventually conclude that the occurrence of a gap is not directly related to the presence of instantons on  $S^2$ ; even in the zero instanton sector, after decompactification, no gap occurs for sufficiently large values of  $\mathcal{A}$ . Only when  $\mathcal{A}$  is small enough, the complete and the zero-instanton solution exhibit similar behaviours. We emphasize that this statement has to be proven, since the limits  $N \rightarrow \infty$  and  $\mathcal{A} \rightarrow 0$  could in principle not commute. For small area, only the term with  $m = 0$  contributes to the summation Eq. (61), and therefore we deduce  $\theta_{cr}^{ML} = 2\sqrt{\mathcal{A}}$ . This is precisely the leading term in the expansion of Eq. (58), so that the two values of  $\theta_{cr}$  coincides at small area. Let us now show that also  $\sigma(\mathcal{A}, \theta)$  Eq. (57) and  $\sigma^{ML}(\mathcal{A}, \theta)$  have a similar behaviour for small  $\mathcal{A}$ . As  $\theta < \theta_{cr}$ , by defining  $\theta = \lambda \theta_{cr}$ , we can write

$$\sigma^{ML} = \frac{1}{\pi\sqrt{\mathcal{A}}} \sqrt{1 - \lambda^2}. \quad (62)$$

Notice that the last factor in Eq. (62) is finite as  $\mathcal{A} \rightarrow 0$ . By comparing Eq. (62) and Eq. (57), we expect that the solutions  $(\hat{x}, \hat{y})$  of Eq. (55) behave for small  $\mathcal{A}$  as  $(-\frac{1}{2} + \frac{a}{\sqrt{\mathcal{A}}}, \frac{b}{\sqrt{\mathcal{A}}})$ ,  $a$  and  $b$  being finite numbers. As a matter of fact, solving the trascendental equation Eq. (55) with this ansatz in mind, we find

$$\begin{aligned} \hat{x}_{\pm} &\simeq -\frac{1}{2} \pm \frac{1}{\sqrt{\mathcal{A}}} \sqrt{1 - \lambda^2} \\ \hat{y} &\simeq \frac{\lambda}{\sqrt{\mathcal{A}}}. \end{aligned} \quad (63)$$

Thus, we come to the remarkable result

$$\sigma = \frac{1}{\pi} \left( \hat{x}_+ + \frac{1}{2} \right) \simeq \frac{1}{\pi\sqrt{\mathcal{A}}} \sqrt{1 - \lambda^2}, \quad (64)$$

which is just Eq. (62).

Its precise meaning is elucidated if we remember that  $\sigma(\mathcal{A}, \theta)$  has a distribution character in the limit  $\mathcal{A} \rightarrow 0$ . After introducing the test function  $\varphi(\theta)$ , and defining

$$(\sigma, \varphi) \equiv \int_{-\theta_{cr}}^{\theta_{cr}} d\theta \varphi(\theta) \sigma(\mathcal{A}, \theta), \quad (65)$$

we get

$$(\sigma, \varphi) \simeq \frac{2}{\pi} \int_{-1}^1 d\lambda \sqrt{1 - \lambda^2} \varphi(\lambda\theta_{cr}) \xrightarrow{\mathcal{A} \rightarrow 0} \varphi(0), \quad (66)$$

which shows indeed that, when  $\mathcal{A} \rightarrow 0$ ,  $\sigma(\mathcal{A}, \theta) \rightarrow \delta(\theta)$  in the topology of distributions, both for the exact and the WML case.

On the other hand, at large areas, the genuinely perturbative solution (*i.e.* the one coming from the equal-time quantization and corresponding to the zero-instanton sector), becomes less and less reliable.

To gain a better insight, we consider again the zero-instanton sector on  $S^2$ , before decompactification. Eq. (22) teaches us that this is easily achieved by replacing  $\mathcal{A}$  with  $\frac{(A-\mathcal{A})\mathcal{A}}{A}$ . In the equatorial condition  $A - \mathcal{A} = \mathcal{A}$ , Eq. (61) becomes

$$\sigma_{S^2}^{ML} = \frac{2}{\pi\sqrt{A}} \sum_m \sqrt{1 - \frac{(2\pi m + \theta)^2}{A}}, \quad -\pi \leq \theta \leq \pi. \quad (67)$$

It is amusing to notice that the critical value for  $A$  is now again  $A_{cr} = \pi^2$  and that, below such a critical value, the ML spectral distribution *exactly* coincides with the one in the weak DK phase on the sphere [24].

Actually, from Eq. (22), we can derive a stronger result; we can indeed follow the evolution of the critical area of the loop as a function of the size of the sphere also for the zero-instanton sector. As a matter of fact, Eq. (61) becomes

$$\sigma^{ML}(\mathcal{A}_{cr}^{ML}, \pi) = \frac{\sqrt{A}}{\pi\sqrt{\mathcal{A}_{cr}^{ML}(A - \mathcal{A}_{cr}^{ML})}} \sqrt{1 - \frac{\pi^2 A}{4\mathcal{A}_{cr}^{ML}(A - \mathcal{A}_{cr}^{ML})}}, \quad (68)$$

leading to

$$\mathcal{A}_{cr}^{ML} = \frac{A}{2} \left[ 1 - \sqrt{1 - \frac{\pi^2}{A}} \right]. \quad (69)$$

Starting from the value  $\mathcal{A}_{cr}^{ML} = \frac{\pi^2}{2}$ , when  $A = \pi^2$ , the same as the one of the exact solution, in the decompactification limit  $A \rightarrow \infty$  we recover the threshold  $\mathcal{A}_{cr}^{ML} = \frac{\pi^2}{4}$ , lower than the one of the exact case ( $\mathcal{A}_{cr} = 4$ ).

## V. CONCLUSIONS

The main concern of this paper was to gain a better insight in the dynamics of  $YM_2$  by considering the class of Wilson loops winding  $n$  times around a closed smooth contour, either on a compact manifold ( $S^2$ ) or on the plane. As already noticed by several authors, thanks to the invariance under area-preserving diffeomorphisms, these loops carry enough information to characterize the theory in the large- $N$  limit.

Our deepest result is probably Eq. (26). It shows a curious interplay between two integral numbers,  $N$  characterizing the internal symmetry group and  $n$  representing the number of windings along the contour. In a geometrical language, the latter controls the displacement of the connection on the base manifold, the former is related to displacements along the group fiber. In two dimensions, the winding  $n$  has essentially a topological character, as it appears in the  $n$ -th power of the group element  $U_C$ ; the Wilson loop can then be interpreted as a generalized Clebsch-Gordan coefficient intertwining different  $U(N)$  representations. This is, we believe, the root of Eq. (26) and, of course, it entails far-reaching consequences. In particular it relates the abelian-like exponentiation for  $U(N)$  when  $n = 1$  to the genuine triviality of the Maxwell theory ( $N = 1$ ) for any  $n$ .

All these features are reproduced in a perturbative context. Actually concrete examples of different colour and geometrical interplays are explicitly exhibited, according to the different expressions used for the vector propagator (either WML or 't Hooft). When the 't Hooft propagator is used the perturbative series leads to the exact result. However, for

$n > 1$ , the Wilson loop feels the non-abelian nature of the theory. The winding number  $n$  probes its colour content. The related light-front vacuum, although simpler than the one in the equal-time quantization, as it automatically takes instanton contributions into account, cannot be considered trivial.

A more intriguing result concerns the limit  $n \rightarrow \infty$  keeping  $n^2\mathcal{A}$  fixed, namely the small-area limit. In such a limit (Eq. (32)), one exactly recovers the contribution of the zero-instanton sector, namely Eq. (23). Intuitively this can be understood by remembering that instantons possess a typical length scale measured by their size. One might then be tempted to conclude that the phase transition at large  $N$  is completely driven by instantons. Unfortunately this characterization is true only for small areas, when instantons cannot contribute. In Sect. IV it is shown that, for areas larger than a critical threshold, the spectral function which characterizes the eigenvalue distribution in the exact solution, when computed retaining only the zero-instanton sector, does not exhibit any gap. At large areas, the genuinely perturbative solution (*i.e.* the one coming from the equal-time quantization and corresponding to the zero-instanton sector), becomes less and less reliable, as expected on a general ground. It is then quite remarkable that the perturbative light-front resummation succeeds in reproducing not only the correct string tension, but also the non-trivial corrections (see Eq. (17)) due to colour-winding factors, the winding number  $n$  carrying the information about the non-abelian topology.

One should perhaps conclude with a comment concerning higher dimensional cases, in particular the dimension  $d = 4$ . We believe that most of our results are typical of the two-dimensional case. Perturbation theory at  $d = 2 + \epsilon$  is discontinuous in the limit  $\epsilon \rightarrow 0$  [5,27]; on the other hand the invariance under area-preserving diffeomorphisms is lost when  $d > 2$ . In a perturbative picture the presence of massless “transverse” degrees of freedom (the “gluons”) forces a causal behaviour upon the relevant Green functions, whereas in the soft (IR) limit they get mixed with the vacuum. The light-front vacuum, which also in two dimensions is far from being trivial, in higher dimensions is likely to be simpler only as far as topological degrees of freedom are concerned. Of course there is no reason why it should

coincide with the physical vacuum since, after confinement, the spectrum is likely to contain only massive excitations. Moreover, to be realistic, “matter” should be introduced, both in the fundamental and in the adjoint representation. Therefore, before going to higher dimensions, our two-dimensional considerations should perhaps be generalized to the case in which “matter” is present. Although many papers have appeared to this regard in the recent literature, we feel that further work is still needed to reach a complete understanding.

## VI. APPENDIX A: $\mathcal{W}_n$ $\mathcal{O}(g^4)$ WITH ‘T HOOFT PRESCRIPTION

In this appendix we explicitly compute  $\mathcal{W}_n$  at order  $\mathcal{O}(g^4)$ . We have seen in Sect. III that at this order all diagrams come with the prefactor given by Eq. (42). We now have to group all possible diagrams in different classes according to their contribution either to  $\text{Tr} [T^a T^a T^b T^b]$  (non-crossed diagrams) or to  $\text{Tr} [T^a T^b T^a T^b]$  (crossed diagrams), and to the area factor. We then have to specify how many of them belong to each class (depending on the number of windings  $n$ ) and the area factor they produce <sup>4</sup>. Such numbers are summarized in the following tables: Table I refers to non-crossed diagrams depicted in Fig. 2, whereas Table II to crossed ones depicted in Fig. 3. Finally, summing up the contributions from all loops, each multiplied by the prefactor (42), the proper trace and area factor, and taking into account the multiplicity, we recover the result announced in (45) for the Wilson loop with  $n$  windings at order  $\mathcal{O}(g^4)$ .

## VII. APPENDIX B

In this appendix we will sketchily show that Eq. (55) admits two solutions and, of these, only one can be encircled by the integration contour. Let us start from Eq. (55), which,

---

<sup>4</sup>Recall it is either  $\frac{1}{2}$  or 1 depending on whether there are nested integrals in the loop variables or not.

after inserting  $t = x + iy$ , reads

$$\frac{1 + x + iy}{x + iy} e^{-\mathcal{A}(x + \frac{1}{2})} e^{i(\theta - \mathcal{A}y)} = 1. \quad (70)$$

The first obvious symmetry to be noticed is  $(x, y, \theta) \rightarrow (x, -y, -\theta)$ . In addition, by taking the absolute value of Eq. (70), the symmetry  $x \rightarrow -x - 1$  is also manifest. Combining Eq. (70) and its complex conjugate, we obtain an equation for the shape of the boundary which separates the region of convergence of Eq. (52) and the forbidden region

$$y^2 = -(x^2 + x + \frac{1}{2}) + (x + \frac{1}{2}) \coth(\mathcal{A}(x + \frac{1}{2})), \quad \text{for } x \neq -\frac{1}{2}. \quad (71)$$

It follows

$$\frac{dy^2}{dx} = -\frac{x + \frac{1}{2}}{\sinh^2(\mathcal{A}(x + \frac{1}{2}))} f(x; \mathcal{A}), \quad (72)$$

where

$$f(x; \mathcal{A}) = \mathcal{A} - \frac{\sinh(\mathcal{A}(2x + 1))}{2x + 1} + 2 \sinh^2(\mathcal{A}(x + \frac{1}{2})). \quad (73)$$

It is easy to check that the same function  $f$  appears in the derivatives of the coordinates  $x$  and  $y$  with respect to  $\theta$ . From Eq. (70) we infer

$$\begin{aligned} \frac{\partial x}{\partial \theta} &= \frac{\partial y}{\partial \theta} \frac{y g(x, y)}{f(x; \mathcal{A})}, \\ \frac{\partial y}{\partial \theta} &= \frac{f(x; \mathcal{A})}{f^2(x; \mathcal{A}) + y^2 g^2(x, y)}, \end{aligned} \quad (74)$$

with

$$g(x, y) = \frac{1}{(x + 1)^2 + y^2} - \frac{1}{x^2 + y^2}.$$

By comparing Eqs. (72), (74) we deduce

$$\begin{aligned} \text{sign} \frac{\partial y}{\partial \theta} &= -\text{sign} \frac{dy^2}{dx} & \text{if } x > -\frac{1}{2}, \\ \text{sign} \frac{\partial y}{\partial \theta} &= \text{sign} \frac{dy^2}{dx} & \text{if } x < -\frac{1}{2}. \end{aligned} \quad (75)$$

We conclude that, if for  $\theta = \theta_0$  a root of Eq. (55) exists, for  $\theta > \theta_0$  its ordinate  $y_r(\theta, \mathcal{A})$  follows the boundary continuously. Moreover, Eq. (70) tells us that for  $\theta = 0$  there are two

roots sitting on the  $x$ -axis ( $y_r = 0$ ), whose  $x$  coordinates are the solutions of the following equation

$$\frac{x+1}{x} = e^{\mathcal{A}\left(x+\frac{1}{2}\right)}. \quad (76)$$

One can check that Eq. (76) admits only two solutions, for any value of  $\mathcal{A}$ , symmetric with respect to the axis  $x = -\frac{1}{2}$ . Clearly, when  $x$  approaches the value  $-\frac{1}{2}$ , the condition  $y^2 \geq 0$  in Eq. (71) can be fulfilled only if  $\mathcal{A} \leq 4$ . Therefore, we start at  $\theta = 0$  with two roots on the real axis which move continuously along the boundary as  $\theta$  increases if  $\mathcal{A} > 4$ , whereas for  $\mathcal{A} \leq 4$  there is a critical value of  $\theta$ , let us call it  $\theta_{cr}$ , for which the two roots reach the axis  $x = -\frac{1}{2}$  and then remain on it, moving in the imaginary direction. Hence a gap is originated, since

$$\sigma(\mathcal{A}, \theta) = 0 \quad \text{for } \theta \geq \theta_{cr}, \quad \mathcal{A} \leq 4.$$

At this stage we present an hand-waving argument to show that only one of the two roots is encircled by the integration contour. Nevertheless a rigorous proof based on a thorough examination of Eq. (53) can be given. Although the region of convergence of Eq. (52) appreciably varies according to the value of  $\mathcal{A}$ , it is always made up of disconnected pieces and the axis  $x = -\frac{1}{2}$  represents a border line between a domain of convergence and a forbidden region. As a consequence, the integration contour, which encircles the origin of the complex plane (lying in the forbidden region), is forced not to cross such an axis and to capture just one of the two roots (remember they are symmetric with respect to the exchange  $x \rightarrow -x - 1$ ). This root in turn and the origin become the two branch points of the logarithm in Eq. (54).

Let us now determine the exact value of  $\theta_{cr}$  in case  $\mathcal{A} < 4$ . The criticality is reached when  $\hat{x} = -\frac{1}{2}$ , so that we evince from Eq. (71)

$$y_{cr} = \pm \sqrt{\frac{1}{\mathcal{A}} - \frac{1}{4}}.$$

Then Eq. (70) becomes



$$\begin{cases} -\frac{1}{2} = \frac{1}{2} \cos(\theta_{cr} - Ay_{cr}) - y_{cr} \sin(\theta_{cr} - Ay_{cr}) \\ y_{cr} = \frac{1}{2} \sin(\theta_{cr} - Ay_{cr}) + y_{cr} \cos(\theta_{cr} - Ay_{cr}) \end{cases} \quad (77)$$

Eventually, by inserting the value of  $y_{cr}$ , the solution is straightforwardly found

$$\theta_{cr} = \sqrt{\mathcal{A} - \frac{\mathcal{A}^2}{4}} + \arccos\left(1 - \frac{\mathcal{A}}{2}\right). \quad (78)$$

**Acknowledgement** Discussions at an early stage of this work with G. Nardelli are acknowledged. One of us (A.B.) wishes to thank Y. Frishman and G. Miller for their hospitality at the Physics Departments of the Weizmann Institute (Rehovot) and of the University of Washington (Seattle), respectively, while part of this work was done.

TABLES

Diagrams	number	area factor
Fig. 1a	$n$	$\frac{1}{2}$
Fig. 1b	$2n(n-1)$	$\frac{1}{2}$
Fig. 1c	$n(n-1)$	$\frac{1}{2}$
Fig. 1d	$\frac{n(n-1)}{2}$	1
Fig. 1e	$\frac{n(n-1)}{2}$	1
Fig. 1f	$n(n-1)(n-2)$	$\frac{1}{2}$
Fig. 1g	$n(n-1)(n-2)$	1
Fig. 1h	$\frac{n(n-1)(n-2)}{2}$	1
Fig. 1i	$\frac{n(n-1)(n-2)(n-3)}{3}$	1

TABLE I. Classes of non-crossed diagrams contributing to  $\mathcal{W}_n \mathcal{O}(g^4)$  with counting and area factor.

Diagrams	number	area factor
Fig. 2a	$2n(n-1)$	$\frac{1}{2}$
Fig. 2b	$n(n-1)(n-2)$	$\frac{1}{2}$
Fig. 2c	$\frac{n(n-1)(n-2)}{2}$	1
Fig. 2d	$\frac{n(n-1)(n-2)(n-3)}{6}$	1

TABLE II. Classes of crossed diagrams contributing to  $\mathcal{W}_n \mathcal{O}(g^4)$  with counting and area factor.

FIGURES

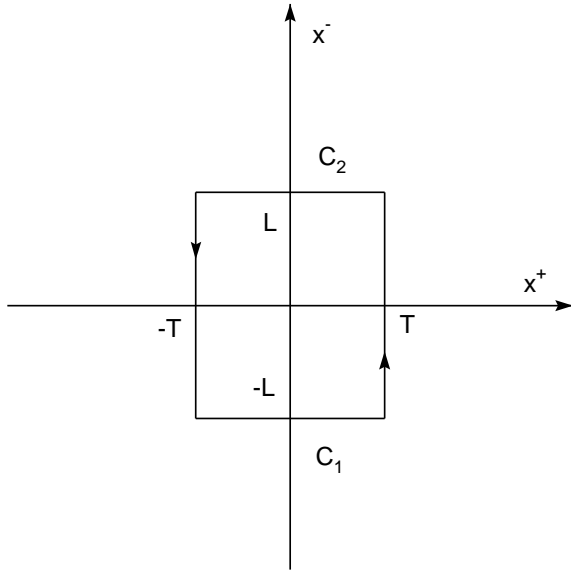
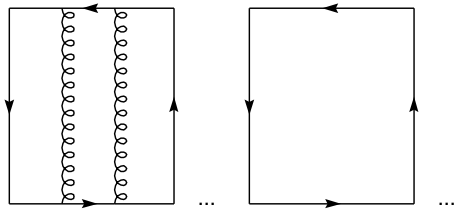
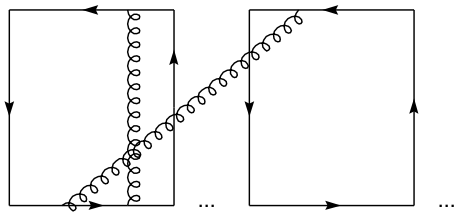


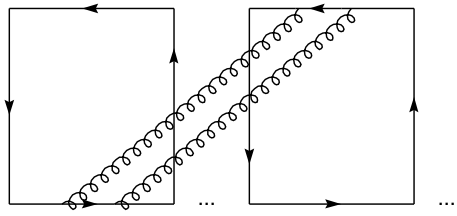
FIG. 1. Contour.



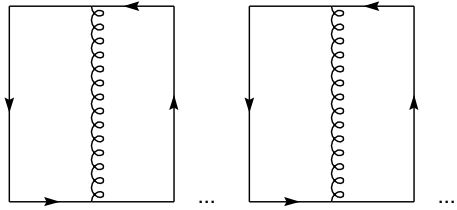
(a)



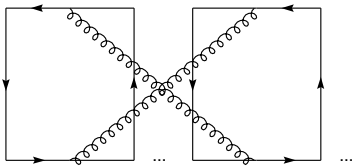
(b)



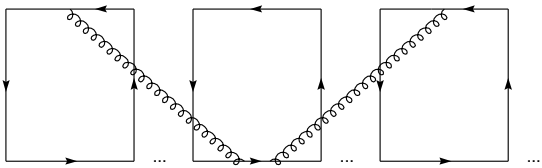
(c)



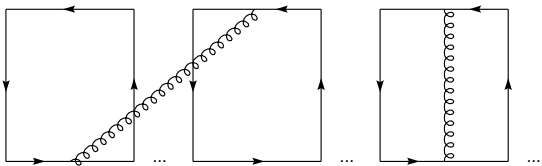
(d)



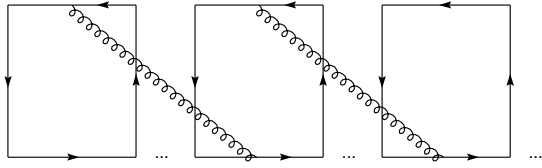
(e)



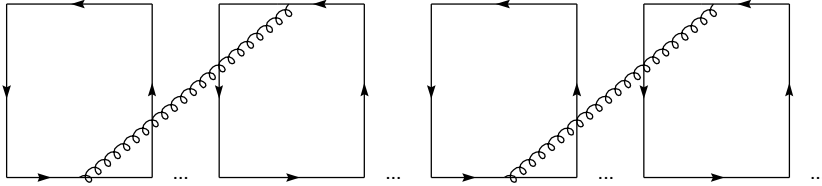
(f)



(g)

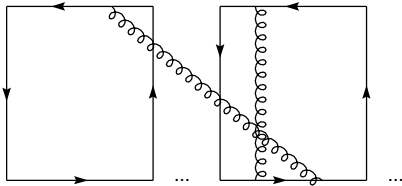


(h)

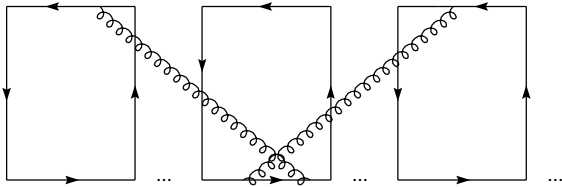


(i)

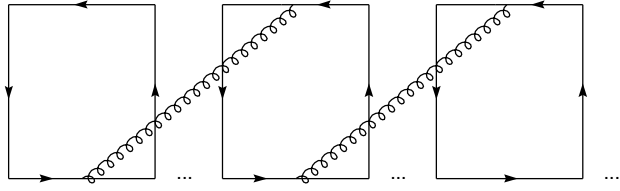
FIG. 2. Non-crossed graphs. The  $i^{\text{th}}$  sheet corresponds to the  $i^{\text{th}}$  winding.



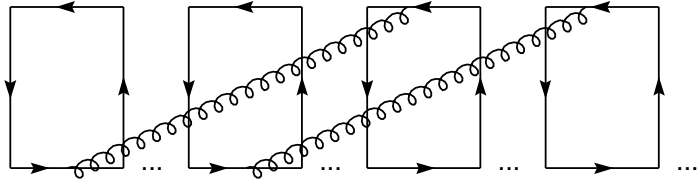
(a)



(b)



(c)



(d)

FIG. 3. Crossed graphs.

## REFERENCES

- [1] N. Seiberg and E. Witten, Nucl.Phys. **B426**, 19 (1994); Erratum *ibid.* **B430**, 485 (1994); *ibid.* **B431**, 484 (1994).
- [2] J.M. Maldacena, Adv. Theor. Math. Phys. **2**, 231 (1998).
- [3] S. Brodsky, Phys. Rep. **301**, 299 (1998) and references therein.
- [4] A.A. Migdal, Sov. Phys. JETP **42**, 413 (1975); B.E. Rusakov, Mod. Phys. Lett. **A5**, 693 (1990).
- [5] A. Bassetto, F. De Biasio and L. Griguolo, Phys. Rev. Lett. **72**, 3141 (1994).
- [6] T.T. Wu, Phys. Lett. **71B**, 142 (1977).
- [7] S. Mandelstam, Nucl. Phys. **B213**, 149 (1983).
- [8] G. Leibbrandt, Phys. Rev. **D29**, 1699 (1984).
- [9] A. Bassetto, M. Dalbosco, I. Lazzizzera and R. Soldati, Phys. Rev. **D31**, 2012 (1985).
- [10] A. Bassetto, G. Nardelli and R. Soldati, *Yang-Mills Theories in Algebraic Non-Covariant Gauges*, World Scientific, Singapore 1991.
- [11] A. Bassetto, I.A. Korchemskaya, G.P. Korchemsky and G. Nardelli, Nucl. Phys. **B408**, 62 (1993); A. Bassetto and M. Ryskin, Phys. Lett. **B316**, (1993); C. Acerbi and A. Bassetto, Phys. Rev. **D49**, 1067 (1994); A. Bassetto, Nucl. Phys. Proc. Suppl. **51C**, 281 (1996); A. Bassetto, G. Heinrich, Z. Kunszt and W. Vogelsang, Phys. Rev. **D58**, 094020 (1998).
- [12] G. 't Hooft, Nucl. Phys. **B75**, 461 (1974).
- [13] A. Bassetto and L. Griguolo, Phys. Lett. **B443**, 325 (1998).
- [14] B. Durhuus and P. Olesen, Nucl. Phys. **B184**, 406 (1981).
- [15] Y.M. Makeenko and A.A. Migdal, Phys. Lett. **88B**, 135 (1979).

- [16] B. Durhuus and P. Olesen, Nucl. Phys. **B184**, 461 (1981).
- [17] V.A. Kazakov and I.K. Kostov, Nucl. Phys. **B176**, 199 (1980); V.A. Kazakov, *ibid.* **179**, 283 (1981).
- [18] N.E. Bralić, Phys. Rev. **D22**, 3090 (1980).
- [19] L. Griguolo, Nucl. Phys. **B547**, 375 (1999).
- [20] P. Rossi, Ann. Phys. **132**, 463 (1981).
- [21] M. Staudacher and W. Krauth, Phys. Rev. **D57**, 2456 (1998).
- [22] D. J. Gross and A. Matytsin, Nucl. Phys. **B437**, 541 (1997).
- [23] E. Witten, Commun. Math. Phys. **141**, 153 (1991) and J. Geom. Phys. **9**, 303 (1992).
- [24] M.R. Douglas and V.A. Kazakov, Phys. Lett. **B319**, 219 (1993).
- [25] M. Caselle, A. D'Adda, L. Magnea and S. Panzeri, *Two dimensional QCD on the sphere and on the cylinder*, in Proceedings of Workshop on High Energy Physics and Cosmology, (Trieste 1993) eds. E.Gava, A.Masiero, K.S.Narain, S.Randjbar-Daemi and Q.Shafi, World Scientific, Singapore, 1994.
- [26] D. J. Gross and A. Matytsin, Nucl. Phys. **B429**, 50 (1994).
- [27] A. Bassetto, R. Begliuomini and G. Nardelli, Nucl. Phys. **B534**, 491 (1998) and Phys. Rev. **D59**, 125005 (1999).